

Effects of Plasma Drag on Low Earth Orbiting Satellites due to Heating of Earth's Atmosphere by Coronal Mass Ejections

Victor U. J. Nwankwo^{1*}, and Sandip Kumar Chakrabarti^{1,2}

victornwankwo@yahoo.com; chakraba@bose.res.in

¹ S. N. Bose National Centre For Basic Sciences, Kolkata 700098, India

² Indian Centre for Space Physics, Kolkata 700084, India

Abstract

Solar events, such as coronal mass ejections (CMEs) and solar flares, heat up the upper atmosphere and near-Earth space environment. Due to this heating and expansion of the outer atmosphere by the energetic ultraviolet, X-ray and particles expelled from the sun, the low Earth-Orbiting satellites (LEOS) become vulnerable to an enhanced drag force by the ions and molecules of the expanded atmosphere. Out of various types of perturbations, Earth directed CMEs play the most significant role. They are more frequent and intense during the active (solar maximum) phase of the sun's approximately 11-year cycle. As we are approaching another solar maximum later in 2013, it may be instructive to analyse the effects of the past solar cycles on the orbiting satellites using the archival data of space environment parameters as indicators. In this paper, we compute the plasma drag on a model LEOS due to the atmospheric heating by CMEs and other solar events as a function of the solar parameters. Using the current forecast on the time and strength of the next solar maximum, we predict how an existing satellite orbit may be affected in the forthcoming years.

Keywords: Solar parameters; Solar cycle; Space weather events; CMEs; orbital decay

*Corresponding author: victornwankwo@yahoo.com

1 Introduction

Solar activity is long known to have a significant influence on the upper atmosphere and the near-Earth space environment which affects modern equipments and consequently human activities on Earth. Solar activity has an approximate 11-year cycle, which includes a stage each of solar maximum and minimum. Normally, the sun emits a continuous stream of energetic particles and electromagnetic radiation which has various time scales and intensities. The major processes of the solar energetic emissions are the solar flares and the coronal mass ejections (CMEs). Both of these processes are sporadic, and are the primary causes of adverse space weather. These processes are more frequent and intense during the solar maximum but less in magnitude and frequency during solar minimum. It has been predicted by NASA [NOAA(2012a)] that the current, i.e., 24th solar cycle will attain its peak later in 2013, typically lasting for about six months. Given that a severe space weather has a direct and generally adverse effects on low earth orbiting satellites (LEOS) on which many human activities depend, it is pertinent to compute the severity of the effects ahead of the events.

The space weather events are natural sources of hazards [IRGC(2010), Lloyd(2010)]. Effects of the space weather on the Earth and space systems include satellite drag [Gopalswamy(2009)]; disruption and damage of modern electric power grids, corrosion of oil/gas pipelines due to geomagnetic induced current (GIC), satellite sensor degradation; radiation threat to crew of high-flying aircraft and astronauts [IRGC(2010), Gopalswamy(2009), NRC(2008)], degradation of precision of Global Positioning System's (GPS) measurement; operational anomalies in satellites, damage of critical electronics and degradation of solar arrays due to exposure to energetic particles during solar particle events (SPE) [NRC(2008), Jibiri et al.(2011)] etc. Secondary effects arise due to inter-dependency of systems on near-Earth space missions. Societal and economic impacts are also part of the resultant risks [IRGC(2010), Lloyd(2010)].

A number of factors determine the effects of the space weather on the satellite orbits. These include the phase of the 11-year solar cycle, the nature of the spacecraft orbit, the local time and the position of the satellite relative to Earth-Sun direction [NOAA(2006a)]. Although impact probabilities (affecting the orbit) increase with the rising phase of the peak, certain effects occur at all the phases (and/or stages) of the cycle. For instance, the Van Allen Radiation Belt (VARB) is a potential threat zone for satellites. The effect is more or less independent of the phase of the cycle. Energetic

particles, such as electrons are present during solar minimum as well and also affects the satellite system. It was reported [NOAA(2006a), Ioannis(2001)] that two Canadian satellites (including Anik E1) experienced debilitating upsets in 1994 at the end of a long duration of adverse condition of the space weather. Similarly, Telsat 410 (AT & T communication satellite) and Galaxy 4 also failed in 1997 and 1998 respectively [Ioannis(2001)]. A notable space weather event that produced significant impact during past solar peak is the Carrington event of September 1859. This is perhaps the largest recorded geomagnetic storm [IRGC(2010), NRC(2008), Lloyd(2010), POST(2010)]. This event significantly disrupted telegraph systems around the world for as long as eight hours. Two other similar events, albeit of lesser magnitude, occurred in March 1989 and in October/November 2003 respectively [IRGC(2010), NRC(2008), Lloyd(2010), Ioannis(2001), POST(2010)]. The former, a geomagnetic storm that resulted to the collapse (in about ninety minutes) of the Hydro-Quebec (Canada) power system, and led to complete blackout of utility grid in North America for about nine hours. The latter event caused long-hour power outage in Sweden, and in UK, temporarily changed the ‘compass north’ by five degrees for six minutes [POST(2010)]. More than 30 satellite anomalies were reported as a consequence of this event, with one of Japan lost completely [Lloyd(2010), POST(2010)].

Because of these plethora of evidences, there are justifiable concerns on the probable impact of the space weather due to the forthcoming solar maximum. In this section, we concentrate on studying the effects of the solar events systematically. In the next Section, we briefly describe major solar events which are taken care of in our study. In §3, we present the method of our analysis. In §4, we present the computation of the average orbital decay due to the solar events in question. In §5, we present our results and discussions. Finally, we make our concluding remarks.

2 Factors affecting Space Weather in solar system

The Sun is clearly the primary cause of space weather condition in the solar system. In a solar wind, a stream of energized charged particles (primarily protons and electrons) constantly flows outward from the solar corona and hits the magnetic corona. A momentary and sudden release of the magnetic energy, also known as the solar flares, and large-scale, high-mass, eruptions of plasma, widely known as the Coronal Mass Ejections, are also created

in the solar corona and are injected into the interplanetary space, which occasionally hits the Earth, especially when they are earth-pointing. Electromagnetic and particle flux radiation emitted during these processes cause adverse conditions in space weather. Among all the events, CMEs are the most damaging, because they may scoop out up to 10^9 tons of magnetized plasma [Gopalswamy(2009)] from the Sun and inject it into the interplanetary space, thereby increasing the chance of its interaction with the Earth. While the solar flares inject energetic particles and radiations into the interplanetary space, CMEs propagate inside the solar wind and drive shock waves, which in turn accelerate energetic particles [Gopalswamy(2009), NOAA(2006b)]. CMEs are sometimes associated with solar flares and prominence eruptions but do also occur without any of the processes. These ejecta interact with the Earth's magnetosphere perturbing it and often causing rapid changes in the Earth's magnetic field. This process result in geomagnetic storms. A CME can reach the earth in about a day or more depending on its speed of propagation [Gopalswamy(2009)]. The mechanism of acceleration and propagation of CMEs are not well understood [Ruffolo(2005), Gopalswamy et al.(2009), Shane & Peter(2005)], though efforts are on to understand them using various models [Gopalswamy et al.(2009)].

3 The Procedure of our analysis

In this work, we study the time variation of different solar parameters as indicators of the Solar activity. We procured archival data for past space weather events and analysed them. We compute the plasma drag on a model satellite in lower earth orbit (LEO) during the events and predict using the solar cycle forecast, as to how the satellite orbit could be affected around the peak of next solar maximum. In addition to the CME catalog [SOHO/LASCO(2012)], three solar parameters were used as tracers of the phase of a solar cycle, They are: a) observed daily solar flux and geomagnetic Ap indices [NOAA(2012b)], b) predicted monthly mean solar flux indices [NOAA(2012c)], and c) sunspot number [NOAA(2012b)]. Our analysis covers approximately two cycles (1995-2019), including a seven-year predicted quantities (2013-2019). We made two-stage analysis and grouped the data according to their anticipated impact level: (i) 1995-2009, assumed to be the period between a solar minimum to the next (min-to-min), and (ii) 1999-2013, assumed to be the period between a solar maximum to the next (max-to-max). Further, we analyzed the data around the last solar maximum and minimum. The grouping is shown in Table 1 (also see, [Pardini et al.(2004), Poole(2002)] below). Our choice of fifteen years interval (between two minima and max-

ima) is not only for convenience, but also because (i) the solar cycle is not strictly of 11-year duration, (ii) occurrence of a seemingly ‘double-peak’ during some solar maximum stage (as could be observed in figure 1b); increases the interval between one peak to the next peak, and (iii) the influence of the ‘extended’ sporadic solar activity after some solar maximum, such as the event of late 2003.

Table 1: Classified/grouped data according to anticipated impact level

Solar flux (F10.7) index				Geomagnetic Ap index	
	Value	Classification	Group	Value	Classification
1	65-99	Average solar activity (ASA)	A	0-14	Quiet/Avg mag. condition (QMC)
2	100-150	Moderate solar activity (MSA)	B	15-29	Active magnetic condition (AMC)
3	151-200	High solar activity (HSA)	C	30-49	Minor storm condition (MnSC)
4	201-250	Very high solar activity (VSA)	D	50-99	Major storm condition (MjSC)
5	251-300	Extreme solar activity (ESA)	E	≥ 100	Severe storm condition (SSC)

Solar flux index (F10.7), monitored at the 10.7 cm wavelength is treated as a measure of the contribution from interactions and subsequent heating of the upper atmosphere by solar energetic particles and ultra-violet (UV) radiation during solar events. The geomagnetic planetary K index (from which the planetary A index is derived) represents the measure of the contribution from the additional atmospheric heating that happens during geomagnetic storms [NOAA(2006a), IRS(1999), Pardini et al.(2004)]. Upper atmospheric expansion is a direct consequence of the heating as measured by these solar parameters. This causes the atmospheric density at higher altitude to increase resulting to an increase in drag on satellites especially those at LEO. The satellite orbit decays and causes its re-entry into the Earth, unless appropriate corrective measures are taken to stabilize its orbital parameters.

4 Computation of orbital decay due to plasma drag

In order to compute the orbital decay of a satellite orbit, we apply a simple atmospheric model equation to begin with, and study the effects of the space environmental parameters (SEP) on it. For concreteness and without any loss of generality, we assumed the satellite with an exposed surface area of a unit square meter (1 m^2) in all directions, to possess a mass of 100kg and orbiting the Earth at an initial injected circular orbit of radius 400km. We

chose a spherical polar co-ordinate system (r, ϕ) having origin $r = 0$ at the center of the Earth and assume that the satellite always remained in the same plane (i.e., $\theta = \text{constant}$). The effects of the drag force were computed from three basic sets of equations. The first set consists of four coupled differential equations.

$$\dot{v}_r = -\frac{GM_e}{r^2} + r\dot{\phi}^2, \quad \dot{r} = v_r, \quad (1)$$

$$\ddot{\phi} = -\frac{1}{2}r\rho\dot{\phi}^2\frac{A_sC_d}{m_s}, \quad \dot{\phi} = v_\phi/r.$$

Here, v_r and v_ϕ are the radial and tangential velocity components respectively. G is the gravitational constant, M_e mass of the Earth, r is the instantaneous radius of the orbit, ρ atmospheric density, A_s is the omni-directional projected area of the satellite, m_s is the mass of the satellite and C_d the drag coefficient at an altitude of r . Note that the drag force has been applied only to the tangential direction, since the velocity is very high only in that direction. The four differential equations are solved by the fourth order Runge-Kutta method to obtain instantaneous positions and velocity components of the satellite in an orbit. To measure the decay of the orbital radius per orbit, we assume that the energy is constant per orbit.

Let E_{total} be the total energy (kinetic and potential) in a orbit. After one revolution, the energy changes to E'_{total} which is given by [USAFA(2012)],

$$E'_{total} = E_{total} - W_{drag}, \quad (2)$$

$$E_{total} = \frac{m_s r v^2 - 2GM_e m_s}{2r}, \quad v = \sqrt{v_r^2 + v_\phi^2},$$

$$W_{drag} = \frac{1}{2}\rho A_s C_d v^2 s, \quad s = 2\pi r,$$

where, W_{drag} is the work done by the drag force per revolution, i.e., after a traversal of s distance. The input parameter ρ in both sets of equations above are to be supplied by the following equation [IRS(1999)],

$$\rho = 6 \times 10^{-10} \exp -\frac{(h - 175)}{H}, \quad (3)$$

where, T (in Kelvin), m and H (in km) are the exospheric temperature (as a function of the solar flux and geomagnetic Ap index), effective atmospheric

molecular mass, and variable scale height respectively. h (km) is the satellite's altitude. These quantities are given by,

$$\begin{aligned} T &= 900 + 2.5(F10.7 - 65) + 1.5(A_p) \\ m &= 27 + 0.012(h - 200); \quad 180 \geq h \geq 500\text{km}; \\ H &= T/m. \end{aligned}$$

5 Statistics of Solar events which affect Satellite Orbits

Figures 1(a-d) show the distribution of solar activity parameters during 1995-2019 period, which include the extrapolated data of 2013-2019 based on present state of the solar activity. In Fig. 1a, we show the daily distribution of the solar flux (left Y-axis) and the geomagnetic Ap Index (right Y-axis) by brown points and blue points respectively. The average values are drawn by red and yellow curves respectively. From the year 2013 onwards (from day number 6580) the data is smooth as they are extrapolated results. The peak in the upcoming solar maximum is clearly shallow than the one of immediate past. The duration of the present cycle is also expected to be shorter. In Fig. 1b, we replot sunspot number and solar flux index (data smoothed over one month) from 1991 to 2019, where the data since 2013 being the predicted value [NOAA(2012c)]. We then superposed the smoothed Geomagnetic Ap Index numbers (right Y-axis). In Fig. 1c, we plot the number of CMEs per day and in Fig. 1d, we plot the linear speed of CMEs (in km/s).

The Figures clearly indicate that the magnetic condition is quieter (QAC) during solar minima but significantly increases during the solar maxima. Once 'quiet', the magnetic activity increase gradually as the solar activity increases, but the mean peak of geomagnetic index does not have a direct correlation with the solar maximum. The fall in magnetic activity is equally gradual and the process last even after the solar maximum is over. It is clear that any of the magnetic conditions as classified in Table 1 (such as, QAC, AMC, MnSC, MjSC or SSC) in the magnetosphere may occur at any stage of the solar cycle but varies in frequency. Solar flux (F10.7) index of VSA and ESA class events rarely occur during the solar minimum (see also Fig. 4d below). Figure 1c showed that the rate of CMEs and the mean linear speed increases significantly around a solar peak, and therefore the

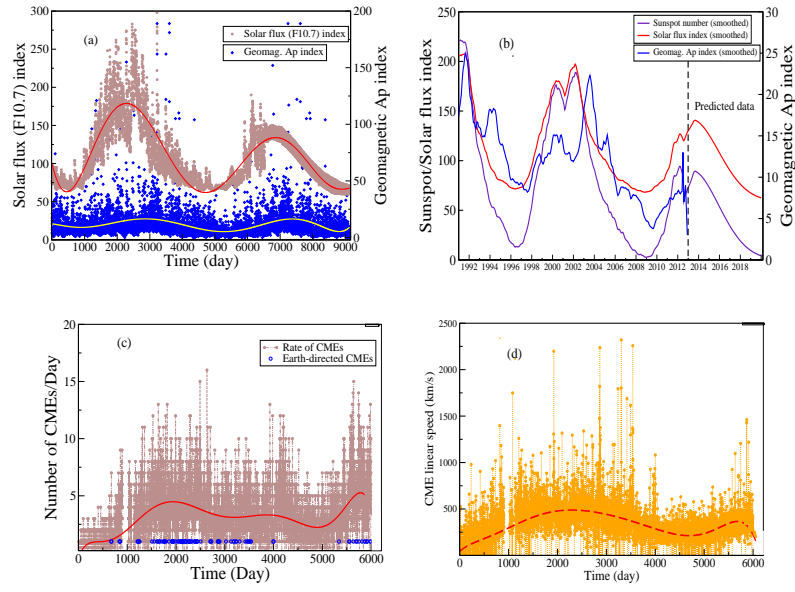


Figure 1: (a) Daily distribution of observed (1995-2012) and predicted (2013-2019) solar flux and geomagnetic Ap index (b) monthly mean distribution of observed (and predicted) sunspot number, solar flux and Ap index (c) Daily rate of CMEs and (d) CME mean linear speed during 1996-2012

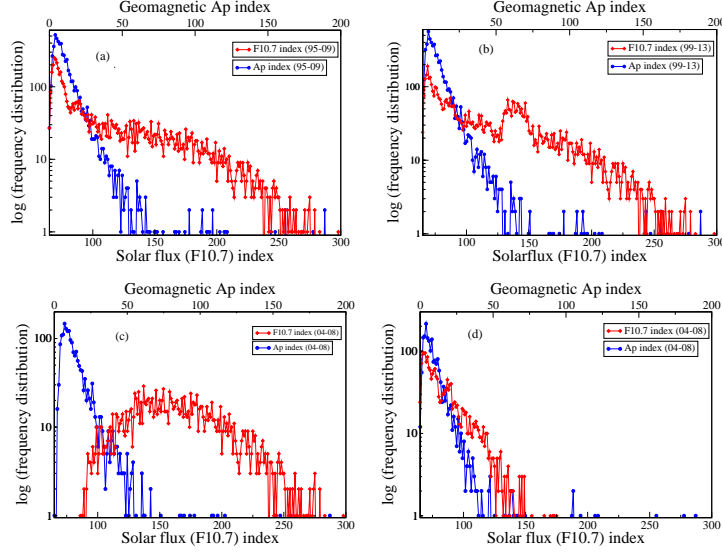


Figure 2: Frequency of occurrence of solar flux and geomagnetic Ap index (a) min-to-min: 1995-2009 (b) max-to-max:1999-2013 (c) around the last solar maximum: 1999-2003 and (d) the last solar minimum: 2004-2008

probability of having more Earth-directed CMEs is also increased. A seemingly ‘double-peaked’ solar maximum has been observed in the past sunspot data [NASA(2012a), SIDC(2012)]. A similar signature is also observed in Figure 1b. Indeed, the actual data shows that 1661, 1500 and 1700 CMEs occurred in 2000, 2001 and 2002 respectively - a clearly convincing example of a ‘double-peak’ in CME number variation. Observed sunspot number and solar flux index (smoothed over one month period) have similar signatures during that period.

The result of the statistical analysis of daily distribution of the solar flux (F10.7) and geomagnetic Ap index is shown in Fig. 2(a-d). The Fig. 2a is drawn for 1995-2009, the period between two minima. Figure 2b is drawn for 1999-2013, the period between two maxima. They are almost identical. Figure 2c is drawn for the period around the last solar maximum 1999-2003. Figure 2d is drawn for the period around the solar minimum 2004-2008. The red points refer to the number of occurrences of a given F10.7 index and the blue points refer to the number of occurrences of a given Geomagnetic Ap Index. Clearly, satellites and space probes would be most vulnerable to drags when both of these indices are simultaneously high. Major space weather events are accompanied by simultaneous occur-

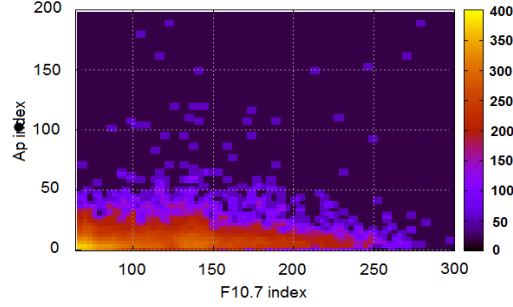


Figure 3: Number of occurrences of solar events as a function of F10.7 & Ap indices. Numbers are colour coded. While the number is high for lower energetic events, those with very high values of solar parameters are sporadic and isolated

rences of VSA ($F10.7 \geq 200$) and SSC ($Ap \geq 100$). The events including July 2000 solar event [NASA(2012b)], April 2001 solar event [SOHO(2012)] and October/November 2003 Halloween storm [NASA(2012c)] during (and around) solar maximum are of this type. In Fig. 3, we draw the frequency of occurrences in colors for any given pair of Ap index and solar F10.7 index. Clearly, number of events having both parameters high are rarer. Three possibilities could increase adverse space weather conditions and ‘magnetospheric’ impacts. They are: (i) High rate of CMEs (8-15/day) with average speed of $\geq 600\text{km/s}$, (ii) low/average rate of CMEs (3-7/day) with high/very high speed of about 1000-2250km/s, and (iii) high rate of CMEs (8-15/day) with high/very high speed, which is the most damaging of all. On 14th July 2000, there were 5 CMEs recorded including a halo CME with speed up to 1674km/s, 7 were recorded on 2nd April 2001 with speed up to 2505km/s and about 24 were recorded between 27th October and 2nd November 2003, with several of them having a speed between 1000 and 2598km/s. Severe geomagnetic storms, both minor and major, also occurred during the solar minimum when ‘persisted’ MSA ($F10.7 \geq 100$) occurred along with SSC ($Ap \geq 100$). Nine severe geomagnetic storm conditions were recorded during 2004 to 2007; three in 2004, three in 2005 and one in 2006. Analysis of the available data showed that 109 and 103 CMEs were respectively recorded in July and November 2004 during which the events occurred. Before the severe storms of 25th and 27th July, a Halo CME with a speed up to 1333km/s occurred on 25th July. Three severe storm conditions were recorded between 8th and 10th November, preceded by three halo CMEs with a speed between 1759 and 3387km/s. Out of the three severe storms recorded in 2005, more

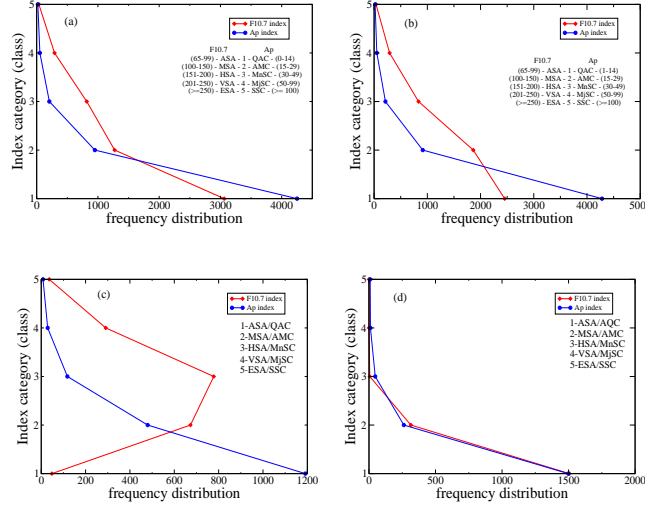


Figure 4: Frequency of occurrence of classified/grouped data (F10.7 & Ap index) (a) min-to-min: 1995-2009 (b) max-to-max: 1999-2013 (c) around last solar maximum: 1999-2003 and (d) last solar minimum: 2004-2008

than seven Halo CMEs preceded the events with a speed between 1194 and 2250km/s. The only severe storm condition recorded in 2006 (on 15th Dec.) was preceded by two Halo CMEs with speeds up to 1774km/s.

In Figs. 4(a-d), we plot the frequency distribution of F10.7 Index and Ap Index in four time slots we considered in Figs. 2(a-d). In Y-axis, we plotted the categories defined in table 1. Note that generally these two indices are correlated, i.e., both the indices have a similar type of variations, though, during a minimum, the correlation is very tight. Only exception is the statistics during the solar maximum - here the number of occurrences of events having very high and very low F10.7 indices is very low indeed, and the most probable event being of category 3 (HSA). The Ap index, however, does to follow this pattern and distribution is monotonic.

6 Computation of Orbital Decay of Satellites

Figure 5(a-b) shows how a model satellite orbit decays with time from an initial altitude of 400km. The average decay in one year under an average condition of each of the five categories of the solar events (as marked in the inset) was computed. The results are shown in Figure 5b. The reduction in height (decay) is about 4, 9, 18, 35 and 75km respectively for a condition of

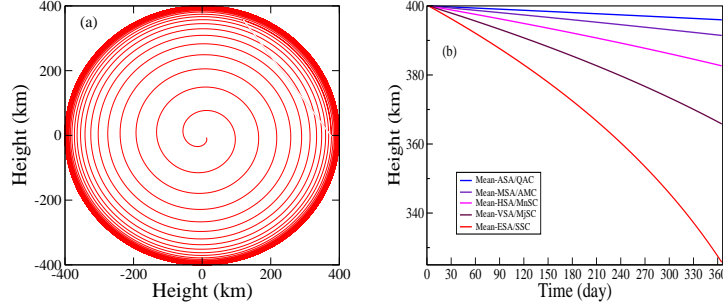


Figure 5: (a) Pictorial representation of decay motion of model satellite from 400km altitude, (b) orbital decay under the influence of mean value of classified/grouped space parameters (F10.7 and Ap index)

average, moderate, high, very high and extreme solar activity respectively. In Fig. 6(a-d), we present the result of two exercises. In Fig. 6a, we present the solar flux (F10.7) and Ap index variation with time in the 1999-2003 period. In Fig. 6b, we present the the number of CMEs/Day and the linear speeds of the CMEs. In Fig. 6c, we show the results of our computation of the atmospheric drag on the satellite using these observed quantities. Five curves show the results computed using the conditions in five successive ‘one year’ interval (indicated) around the last solar maximum. The boxes in Fig. 6c, drawn around the regions of rapid decay in the orbits correspond to the major flare events presented in Figs. 6(a-b) by vertical boxes. In comparison, if we had chosen the data from a period of solar minimum, the results of decay in the period 2004-2008 would have been as shown in Fig. 6d. It is clear that in the period of solar minimum, the orbital decay per year is about half of what we obtain using parameters of the period of solar maximum.

It is interesting to carry out an exercise to study the dependency of the fate of a satellite orbit on the strength of the solar maximum. For the sake of concreteness, we compare two cases: (a) three year period during the last maximum, i.e., 2000-2002 and (b) three year period during the (predicted) upcoming maximum, i.e., 2012-2014. Figures 7(a-b) show the frequency distributions with Gaussian fits of solar flux index for 3-year observed data during the last solar maximum (2000-2002) and emerging (observed + predicted) solar maximum (2012-2014) respectively. Values of F10.7 around 170 were the more frequent during last maximum, and during the next maximum about 136. The respective mean values of (F10.7, Ap) pairs are about (180,14) and (132,13) respectively (we assumed Ap 13 during the next peak).

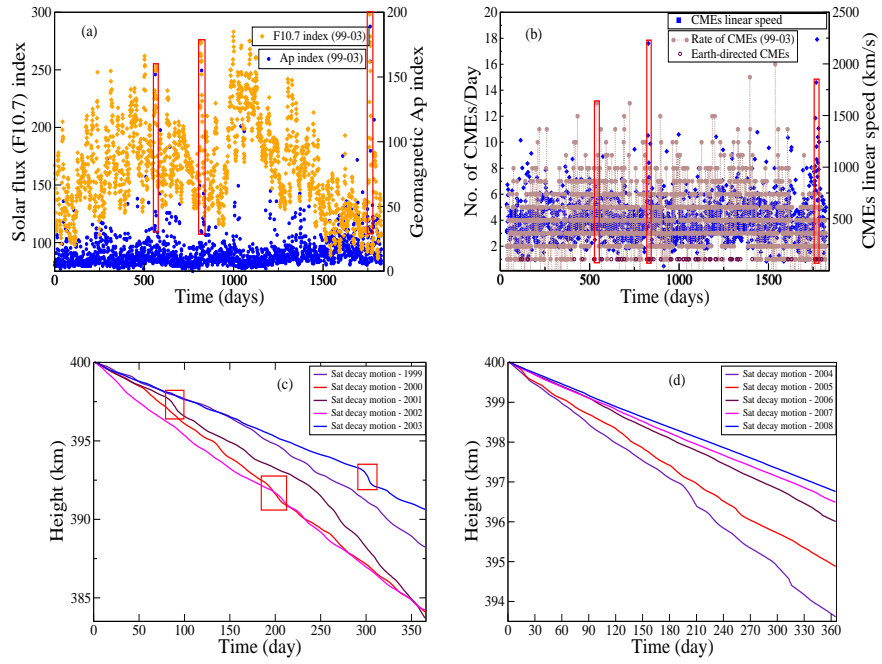


Figure 6: 5-year daily distribution of (a) F10.7 and Ap index and (b) daily CME rate and mean linear speed, around last solar maximum with highlight of data around report dates of major solar events, (c) Satellite's orbital decay in one year interval during 1999-2003 (d) Satellite's orbital decay in one year interval during last solar minimum, 2004-2008

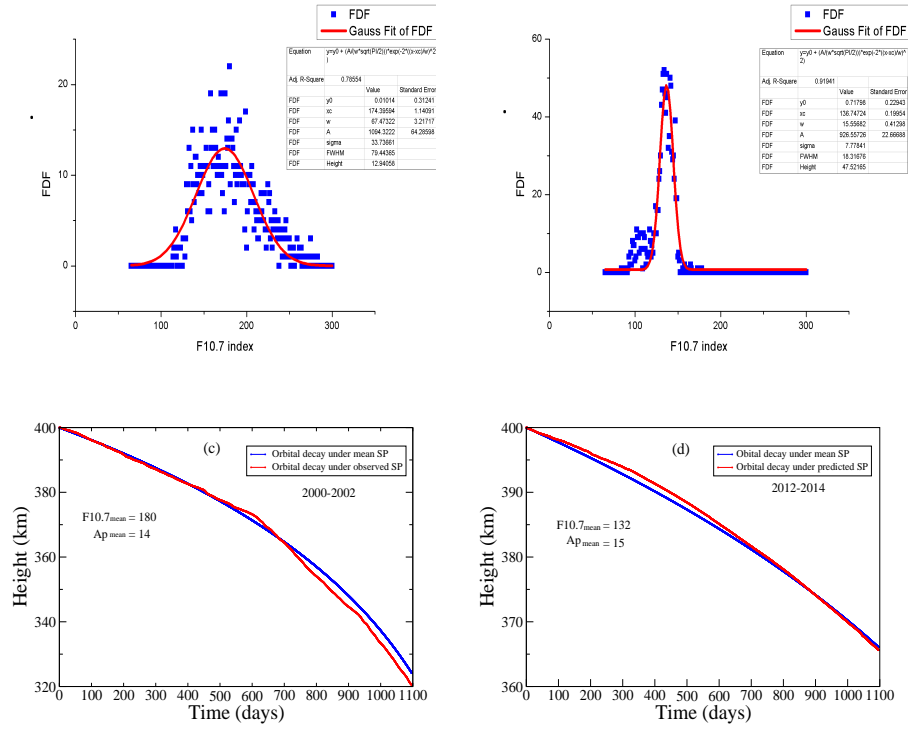


Figure 7: Frequency distribution with Gaussian fit of F10.7 index during (a) last solar maximum, 2000-2002 and (b) around next predicted maximum, 2012-2014 (c) corresponding satellite's orbital decay motion during 2000-2002 and (d) 2012-2014

The results of the corresponding orbital decays under the influence of these parameters are shown in Figs. 7(c-d). It is clear that the expected (F10.7, Ap) being less severe during the next peak, the effects of drag will be milder than the last solar maximum. The mean solar index for the two maxima fall in HSA and MSA categories respectively. Their average decay (in orbit) is about 80km and 35km, corresponding to 20% and 8.75% drop in altitude within a period of three years. The predicted decay, however, excludes contribution from any possible major events during the period. In fact, we estimate that if we assume solar events similar to those of 2000, 2001 and 2003 in the next solar maximum, then in addition to the average effect we computed above (Fig. 7d), we would have at least 2.5% drag effect in excess of the average effect we presented above. Thus we predict that the net plasma drag effect on the orbital decay would be about 11.25% during the next solar maximum.

7 Conclusion

In the present paper, we studied the effects of adverse space weather condition induced by solar events, especially the solar flares and coronal mass ejections on the orbital decay of low earth satellite orbits. We clearly show that the result strongly depends on the phase of the solar cycle. First we studied the statistics of the F10.7 flux index and the Ap index since 1999 and systematically tracked the evolution of an hypothetical satellite in different phases of the solar cycle. Not surprisingly, we found that the effects in the last solar maximum was very severe, while expected effects occurring from the ongoing cycle would be almost half as severe as the previous one. We showed that a major CME event can cause sufficient heating and expansion of the atmosphere so that the orbital radius may go down by a few km in a single event.

Our analysis of statistics of solar events indicates that all types of magnetic conditions, such as, QAC, AMC, MnSC, MjSC and SSC, in the magnetosphere can occur during any stage of the cycle. While QAC category events may occur at any phase of the cycle, the geomagnetic activity could be significantly high during a solar maximum such as the past cycle (1999-2003). We find that during the last solar maximum, QAC was lower by about 20%, while AMC, MnSC and MjSC were higher by about 46%, 60% and 62% respectively as compared to the solar minimum stage (2004-2008). Naturally, we find that a satellite deployed during a solar minimum has higher chance of survival.

Based on estimations of the decay, we find that three types of space

weather conditions are potentially harmful to any space probe. (i) High rate of CMEs ($8 - 15/\text{day}$) with an average speed of $\geq 600\text{km/s}$; (ii) low/average rate of CMEs ($3 - 7/\text{day}$) with a high to very high speed of about $1000 - 2250\text{km/s}$; or, (iii) high rate of CMEs ($8 - 15/\text{day}$) with high/very high speed. We have also observed a ‘double-peak’ feature during the period of solar maximum of a solar cycle. This means that the satellites are likely to be harshly affected for a longer period of time. One of our interesting findings is that for a typical satellite launched at a height of 400km , the plasma drag could cause up to 11.25% decay of its orbit during the upcoming solar maximum, with as much as about 2.5% contribution coming from major CMEs.

Acknowledgment

VUN acknowledges TWAS/ICTP, Trieste, Italy and the S.N. Bose National Centre For Basics Sciences for the post graduate fellowship during which this work was done.

References

- [Gopalswamy(2009)] Gopalswamy N., *Coronal Mass Ejections and Space Weather*. Climate and Weather of the Sun System (CAWSES), TERRAPUB, Tokyo, pp 77-118, 2009
- [Gopalswamy et al.(2009)] Gopalswamy N., Yashiro S., Michalek G., Vourlidas A., Freeland S. and Howard A., 2009, *The SOHO/LASCO CME Catalog*. Earth, Moon and Planets, 104(1-4), pp 295-313, 2009
- [Ioannis(2001)] Ioannis A. D., *Space storms, Ring Current and Space-atmosphere Coupling*. Space Storms and Weather Hazard, NATO Science Series, 38, pp 1-42, 2001
- [IRGC(2010)] IRGC, *Severe Space Weather: solar storms* International Risk Governance Council. IRGC's project on Emerging Risk, 2010
- [IRS(1999)] IRS Radio & Space Services, *Satellite Orbital Decay Calculations*. Australian Space Weather Agency, Sydney, 1999
- [Jibiri et al.(2011)] Jibiri N. N., Nwankwo V. U. J., and Kio M., *Determination of Stopping Power and Failure-time of Spacecraft Components due to Proton Interaction Using GOES 11 Acquisition Data*. International Journal of Engineering Science & Technology (IJEST), 3(8), pp 6532-3542, 2011
- [NASA(2012a)] NASA, 2012a, *The Resurgent Sun*.
http://science.nasa.gov/science-news/science-at-nasa/2002/18jan_solarback/
- [NASA(2012b)] NASA, 2012b, *A Solar Radiation Storm*. NASA Science News.
http://science.nasa.gov/science-news/science-at-nasa/2000/ast14jul_2m/
- [NASA(2012c)] NASA, 2012c, *Halloween Storms of 2003 Still the Scariest*.
www.nasa.gov/topics/solarsystem/features/halloween_storms.html
- [NOAA(2006a)] NOAA, 2006a, *Satellites and Space Weather*.
www.swpc.noaa.gov/info/satellites.html, 2006
- [NOAA(2006b)] NOAA, 2006b, *Space Weather? What Impact do Solar Flares have on Human Activities?:* hesperia.gsfc.nasa.gov/sftheory/spaceweather.htm
- [NOAA(2012a)] NOAA, 2012a, *Solar Cycle Progression*. NOAA Space Weather Prediction Center.
<http://www.swpc.noaa.gov/SolarCycle/>

- [NOAA(2012b)] NOAA, 2012b, *Solar Particle and Geomagnetic Indices*.
www.swpc.noaa.gov/ftpmenu/indices/old_indices.html
- [NOAA(2012c)] NOAA, 2012c, *Predicted Sunspot Number And Radio Flux Values With Expected Ranges*.
www.swpc.noaa.gov/ftplib/weekly/Predict.txt
- [NRC(2008)] NRC, *Severe Space Weather Events - Understanding Societal and Economic Impacts* A Workshop Report. The National Academies Press, Washington DC, 2008
- [Pardini et al.(2004)] Pardini C., Tobiska K., and Luciano A., *Analysis of the orbital decay of spherical satellites using different solar flux proxies and atmospheric density models*. Advance in Space Research, 37(2), pp 392-400, 2004
- [Poole(2002)] Poole L., *Understanding Solar Indices*. NASA, G3YWX, pp 38-40, 2002
- [POST(2010)] POST, *Space Weather*. POST-NOTE 361. The Parliamentary Office of Science and Technology, Millbank, London, 2010
- [Lloyd(2010)] RAL Space, *Space Weather: It's Impacts on Earth and Implications for Business* Lloyd's 360° Risk Insight. London, pp 1-32, 2010
- [Ruffolo(2005)] Ruffolo D., *Transport and Acceleration of Solar Energetic Particles from Coronal Mass Ejection shocks*. Coronal and Stellar Mass Ejections. International Astronomical Union, Precedings IAU Symposium, 226, pp 319-329, 2005
- [Shane & Peter(2005)] Shane M. A. and Gallagher T. P., *Solar Wind Drag and the Kinematics of Interplanetary Coronal Mass Ejections*. The Astronomical Journal Letter, 724, L127-L132, 2005
- [SIDC(2012)] SIDC, *Sunspot index graphics*. Solar Influences Data Analysis Center.
http://www.sidc.be/sunspot-index-graphics/sidc_graphics.php
- [SOHO/LASCO(2012)] SOHO/LASCO, *SOHO LASCO CME CATALOG*.
http://cdaw.gsfc.nasa.gov/CME_list
- [SOHO(2012)] SOHO, *Solar and Heliospheric Observatory*.
sohowww.nascom.nasa.gov/hotshots/X17

[USAFA(2012)] US Air force Academy, *How to Keep a Satellite in Orbit*.
US Air force Academy Laboratory Exercise. *cosmos.phy.tufts.edu/~*
zirbel/laboratories/Satellite.pdf